PostScript file created: January 10, 2012; time 141 minutes

LONG- AND SHORT-TERM EARTHQUAKE FORECASTS DURING THE TOHOKU SEQUENCE

Yan Y. Kagan and David D. Jackson

Department of Earth and Space Sciences, University of California,

Los Angeles, California 90095-1567, USA;

Emails: ykagan@ucla.edu, david.d.jackson@ucla.edu

Abstract. We consider two issues related to the 2011 Tohoku mega-earthquake: (1) what is the repeat time for the largest earthquakes in this area, and (2) what are the possibilities of numerical short-term forecasts during the 2011 earthquake sequence in the Tohoku area. Starting in 1999 we have carried out long- and short-term forecasts for Japan and the surrounding areas using the GCMT catalog. The forecasts predict the earthquake rate per area, time, magnitude unit and earthquake focal mechanisms. Long-term forecasts indicate that the repeat time for the m9 earthquake in the Tohoku area is of the order of 350 years. We have archived several forecasts made before and after the Tohoku earthquake. The long-term rate estimates indicate that, as expected, the forecasted rate changed only by a few percent after the Tohoku earthquake, whereas due to the foreshocks, the short-term rate increased by a factor of more than 100 before the mainshock event as compared to the long-term rate. After the Tohoku mega-earthquake the rate increased by a factor of more than 1000. These results suggest that an operational earthquake forecasting strategy needs to be developed to take the increase of the short-term rates into account.

Short running title: Tohoku earthquake prediction

Key words:

Probabilistic forecasting; Probability distributions; Earthquake interaction, forecasting, and prediction; Statistical seismology; Time-independent and time-dependent forecasts; Forecast testing; Subduction zones; Maximum/corner magnitude.

1 Introduction

The Tohoku, Japan, magnitude 9.1 earthquake (11 March 2011) and the ensuing tsunami near the east coast of the island of Honshu caused nearly 20,000 deaths and more than 300 billion dollars in damage, resulting in the worst natural disaster ever recorded (Hayes *et al.*, 2011; Simons *et al.*, 2011; Geller, 2011; Stein *et al.*, 2011).

Several quantitative estimates of maximum possible earthquakes in subduction zones had been published before the Tohoku event (Kagan, 1997a; Kagan and Jackson, 1994; Bird and Kagan, 2004; Kagan *et al.*, 2010). In these publications the maximum size of these earthquakes was determined to be within a range $m8.5$ – $m9.6$. Two quantitative methods have been deployed to estimate the maximum size of an earthquake: a statistical determination of the magnitude–moment/frequency parameters and a moment conservation principle. The former technique employs standard statistical parameter estimation to evaluate two parameters of the earthquake size distribution: the b-value and the maximum magnitude (Kagan, 2002a; 2002b). The second method works by comparing the estimates of tectonic deformation at plate boundaries with a similar estimate of the seismic moment release (Kagan, 1997a).

The statistical estimate of the maximum magnitude for global earthquakes, including subduction zones and other tectonic regions, yielded the values $m_{\max} \approx 8.3$ (Kagan and Jackson, 1994; 2000). The moment conservation provided an estimate for subduction zones $m_{\max} = 8.5$ – 8.7 ± 0.3 (Kagan, 1997a; 1999; 2002b). The most important result by Kagan

(1997a) is that the maximum earthquake size is the same, at least statistically, for all the studied subduction zones. Combined with the estimate of $m_{\max} = 9.6$ based on the analysis of global seismicity (Bird and Kagan, 2004), this implies that for all major subduction zones the maximum earthquake magnitude should be greater than 9.0 (Kagan and Jackson, 2011b).

Our forecasting technique is to establish a statistical model that fits the catalog of earthquake times, locations, and seismic moments, and subsequently to base forecasts on this model. While most components of the model have been tested (Kagan and Knopoff, 1987; Kagan, 1991; Jackson and Kagan, 1999; Kagan and Jackson, 2000; Kagan *et al.*, 2010), some require further exploration and can be modified as our research progresses.

Our previous forecast model was based on constructing a map of smoothed rates of past earthquakes. We used the Global Centroid Moment Tensor catalog (Ekström *et al.*, 2005, referred to subsequently as GCMT) because it employs relatively consistent methods and lists tensor focal mechanisms. The focal mechanisms allow us to estimate the fault plane orientation for past earthquakes, through which we can identify a preferred direction for future events. Using the forecasted tensor focal mechanism, it may be possible to calculate an ensemble of seismograms for each point of interest on the Earth's surface.

In Section 2 we consider two statistical distributions for the earthquake moment magnitude and show the magnitude-frequency relations for the Tohoku area. We evaluate the approximate recurrence interval for a $m \geq 9.0$ earthquake for the Tohoku area of the order of 350 years (Section 3). Sections 3 and 4 show the long- and short-term earthquake forecasts during the Tohoku sequence. Section 4 illustrates the possibility of an operational type calculation of short-term earthquake rates for short intervals (a few days) after a major earthquake exceeding the long-term rates by 100–1000 times.

2 Earthquake size distribution

We studied earthquake distributions and clustering for the global CMT catalog of moment tensor inversions compiled by the GCMT group (Ekström *et al.*, 2005; Ekström, 2007; Nettles *et al.*, 2011). The present catalog contains more than 33,000 earthquake entries for the period 1977/1/1 to 2010/12/31. The earthquake size is characterized by a scalar seismic moment M.

In analyzing earthquakes here we use the scalar seismic moment M directly, but for easy comparison and display we convert it into an approximate moment magnitude using the relationship (Hanks, 1992)

$$m_W \;=\; \frac{2}{3}\,(\,\log_{10} M - C\,)\,, \tag{1}$$

where $C = 9.0$, if moment M is measured in Newton m (Nm), and $C = 16.0$ for moment M expressed in *dyne-cm* as in the GCMT catalog. Since we are using the moment magnitude almost exclusively, later we omit the subscript in m_W. Unless specifically indicated, we use the moment magnitude calculated as in (1) with the scalar seismic moment from the GCMT catalog.

The earthquake size distribution is usually described by the G-R (Gutenberg and Richter, 1954) magnitude-frequency relation

$$\lg N(m) = a - b\,m\,, \tag{2}$$

where $N(m)$ is the number of earthquakes with magnitude $\geq m$, and a and b are parameters: a characterizes seismic activity or earthquake productivity of a region and b describes the relation between small and large earthquake numbers, $b \approx 1$.

The tapered G-R (TGR) distribution includes an exponential roll-off of frequency for moments near and above a value called the corner moment (Kagan, 2002a). The taper ensures that the total moment rate is finite, and the value of the total moment rate depends

strongly on the corner magnitude. For magnitudes, the tapered G-R relation can be written as

$$\log_{10} N(m) \;=\; \log_{10} a \;-\; b\,(m - m_t) \;+\; \frac{1}{\log(10)} \left[10^{1.5\,(m_t - m_c)} - 10^{1.5\,(m - m_c)}\right], \qquad (3)$$

where m_t is the threshold magnitude: the smallest magnitude above which the catalogue can be considered to be complete, m_c being s the corner magnitude. For the standard two-parameter G-R distribution (2), the last two terms in the right-hand part of (3) are zero ($m_c \to \infty$).

In Fig. 1 we show the moment-frequency curves for shallow earthquakes (the depth is less or equal to 70 km) in the Tohoku area (35-40° N, 140-146° E). The largest earthquake during this period was $m7.68$, thus a low statistical value for the corner magnitude ($m_c^s = 7.8$) is needed to approximate the distribution, whereas the moment conservation principle yielded the value $m_c^m = 9.3$.

Fig. 2 demonstrates why the values of the maximum magnitude determined by historical accounts and even by the standard statistical evaluation method are often grossly biased downward, especially for small time-space intervals, as we see in Fig. 1. After the Tohoku mega-earthquake ($m9.15$) the statistical estimate of the corner magnitude changed drastically ($m_c^s = 10.97$). The lower 95% confidence limit estimate of the corner magnitude is $m8.9$. At the same time, the moment conservation value practically remained the same, i.e., $m_c^m = 9.3$.

3 Long-term earthquake forecasts during the Tohoku sequence

Since 1977 we developed statistical models of seismicity which fit a catalog of earthquake times, locations, and seismic moments; and subsequently we base our forecasts on these mod-

els. The forecasts are produced in two formats: long- and short-term (Kagan and Knopoff, 1977; Kagan and Jackson, 1994; Jackson and Kagan, 1999; Kagan and Jackson, 2000; 2011a) and presently they predict the earthquake rate per area, time, magnitude unit, and focal mechanism. Several earthquake catalogs are used in our forecasts, the GCMT catalog was used most frequently as it employs relatively consistent methods and reports tensor focal mechanisms. The forecasts including those for the north-west Pacific area covering Japan, are posted on our Web site: http://eq.ess.ucla.edu/∼kagan/predictions_index.html .

Figs. 3 and 4 show long-term forecasts for the north-west Pacific area; one forecast is calculated before the 2011 Tohoku sequence started, the other one week after the mega-earthquake. These forecasts are calculated around midnight Los Angeles time. Their description can be found in our publications (Jackson and Kagan, 1999; Kagan and Jackson, 1994; 2000; 2011). There is little difference between these forecasts – long-term forecasts do not depend strongly on current events. Plate 1 in Kagan and Jackson (1994) and Fig. 8a in Kagan and Jackson (2000) display previous forecasts for the same region. Appearance of both plots is similar to Figs. 3 and 4.

In Table 1, we display earthquake forecast rates around the epicenter of the m7.4 Tohoku foreshock. The ratio of the short- to long-term rates (the last column) rises sharply both after the foreshock and after the mainshock. Conclusions similar to those in the previous paragraph can be drawn from Table 1: the maximum long-term rates change only by a few tens of a percent. The predicted focal mechanisms are also essentially the same for the center of the focal area.

To calculate the earthquake long-term rates for the extended area we can integrate the tables over the desired surface, or as a better option, calculate an ensemble of the seismograms for each point of interest on the Earth's surface. This can be accomplished by using a forecasted tensor focal mechanism, such as shown in Table 1. These seismograms can be used

to calculate probable damage to any structure due to earthquake waves. Such calculations are superior in usefulness to earthquake hazard maps (such as the Japanese map shown, for example, by Geller, 2011 and by Stein *et al.*, 2011). Hazard maps display an intensity of shaking estimated for one particular wave period, whereas synthetic seismograms allow calculating a probability of any structural damage or collapse, depending on the structure's mechanical properties.

Another advantage of earthquake rate forecasts is that they are easily tested for effectiveness (Kagan and Jackson, 2000; 2011) by comparing their predictions with future earthquakes. This testing information is readily available from earthquake catalogs. Hazard maps are more difficult to verify; data on the ground motion intensity are more scarce, especially in the less populated territories. Moreover, these maps may fail for two reasons: an incorrect seismicity model or an incorrect attenuation relation, thus it is difficult to find out the cause of poor performance.

As an illustration, using simple methods we make an approximate estimate of the long-term recurrence rate for large earthquakes in the Tohoku area. In the GCMT catalog, the number of earthquakes with $M \geq 5.8$ in a spherical rectangle 35-40° N, 140-146° E, covering the rupture area of the Tohoku event, is 109 for years 1977-2010 (Fig. 1). If we assume that the corner magnitude is well above $m9.0$ (similar to $m9.6$ for subduction zones, see Bird and Kagan, 2004), the repeat time for the $m9$ and larger events in this rectangle depends on the assumed b-value and is between 300 and 370 years.

Uchida and Matsuzawa (2011) suggest a recurrence interval for $m9$ events 260-880 years. Simons *et al.* (2011) propose a 500-1000 year interval. This interval estimate is partly based on the observation of the Jogan earthquake of 13 July 869 and its tsunami. Even if we assume that this Jogan event was similar in magnitude to the 2011 earthquake and no other such earthquakes have occurred meanwhile (see more discussion in Koketsu and Yokota,

2011), for the Poisson occurrence the probability of such an interval is of the order 3-5%. Moreover, the observation of only one inter-event interval does not constrain the recurrence time of these mega-earthquakes in a really meaningful way; the interval can be as small as a few hundred years or as large as tens of thousands of years. Only the moment conservation principle and the tapered G-R distribution (TGR) distribution provide a reasonable estimate for this interval.

4 Short-term forecasts

Figs. 5–8 display short-term forecasts for the north-west Pacific area produced during the initial period of the Tohoku sequence. Fig. 5, calculated before $m7.4$ foreshock, shows a few weakly 'red' spots in those places where earthquakes occurred during the previous weeks and months. The short-term rate in these spots is usually of the order of a few percent or a few tens of a percent compared to the long-term rate (see also Table 1).

The predicted earthquake rates in the neighbourhood of the future Tohoku event increased strongly with the occurrence of a $m7.4$ foreshock (Fig. 6). As Table 1 demonstrate, just before the Tohoku earthquake, the forecasted rate was about 100 times higher than the long-term rate.

The area of significantly increased probability covers the northern part of the Honshu Island following the Tohoku mega-earthquake occurrence (Fig. 7). The size of the area hardly decreased one week later (Fig. 8) mostly due to the Tohoku aftershocks.

Although only around 5-10% few shallow earthquakes are preceded by foreshocks, the results shown in Figs. 5–8 suggest that an operational earthquake forecasting strategy needs to be developed (Jordan and Jones, 2010; van Stiphout *et al.*, 2010; Jordan *et al.*, 2011) to take the increase of short-term rates into account.

5 Discussion

It is commonly believed that after a large earthquake the focal area of an earthquake "has been destressed" (see, for example, Matthews *et al.*, 2002) thus lowering the probability of a new large event in this place, though it can increase in nearby zones. This reasoning goes back to the flawed seismic gap/characteristic earthquake model (Jackson and Kagan, 2011). Kagan and Jackson (1999) showed that earthquakes as large as 7.5 and larger often occur in practically the same area soon after the occurrence of a previous earthquake. Table 2 displays pairs of shallow earthquakes $m \geq 7.5$ epicentroid of which are closer than their focal zone size (an update of Table 1 by Kagan and Jackson, 1999, or Table 1 by Kagan, 2011). The Table includes three earthquake pairs (see # 3, 24, 25) of the Tohoku sequence and demonstrates that strong shocks tend to repeat in the focal zones of previous events. Michael (2011) shows that earthquakes as large as $m8.5$ are clustered in time and space, thus an occurrence of such a big event does not protect its focal area from the giant next shock.

Stein *et al.* (2011) suggest the following forecast requirements: ideally a forecast should anticipate total economic and casualty losses due to earthquakes. Over a relatively short time period, earthquake damage would seemingly reach the maximum not for the rare very large events, but for the $m7 - m8$ shocks (England and Jackson, 2011). But over long-term, expected or average losses would peak for the largest $m8 - m9$ events; though their rates are low, the total average damage for one event increases faster than the probability of these earthquakes decreases. Since the expected economic and other losses peak for the strongest earthquakes (Kagan, 1997b), it is more important to predict disastrous earthquakes than small ones. However, the loss calculations (Molchan and Kagan, 1992; Kagan, 1997b) are very uncertain, because major losses are often caused by unexpected secondary earthquake effects. Therefore, a prediction of the largest earthquakes is important, hence prediction

schemes that do not specify the earthquake size are of restricted practical use. However, if the maximum earthquake is over-predicted, it diverts resources unnecessarily (Stein *et al.*, 2011).

Any forecast scheme that extrapolates the past instrumental seismicity record would predict future moderate earthquakes reasonably well. However as the history of the Tohoku area shows, we need a different tool to forecast the largest events. In our forecasts we consider the earthquake rate to be independent of the earthquake size distribution, so the latter needs to be specified separately.

As indicated earlier, the seismic moment conservation principle can provide an answer to the above questions. The general idea of the moment conservation was suggested some time ago (Brune, 1968; Wyss, 1973). However, without the knowledge of the earthquake size distribution, the calculation of the maximum earthquake moment size ($m_{\max}$) is still difficult and leads to uncertain or contradictory results. The classical G-R relation is not helpful in this respect because it lacks the specification of $m_{\max}$. Only a modification of the G-R law, that introduces the limiting upper moment could provide a tool to quantitatively derive $m_{\max}$ or its variants. Kagan and Jackson (2000) and Kagan (2002a, 2002b) propose such distributions defined by two parameters, β and variants of $m_{\max}$.

The application of these distributions allows us also to solve the problem of evaluating the recurrence period for these large earthquakes. Determining the maximum earthquake size either by historical/instrumental observations or by the qualitative analogies does not provide such an estimate: a similar earthquake may occur hundreds or tens of thousand years later. Fig. 1 shows how using statistical distributions may facilitate such calculations.

As we discussed in Kagan and Jackson (2011b), the moment conservation principle allows to quantitatively determine the maximum earthquake size. In this respect area-specific calculations provide a more precise size evaluation for many tectonic zones and, most im-

portantly to show that the subduction zones could have the same maximum earthquake size (Kagan, 1997a). Although the determination of $m_{\max}$ by comparing tectonic and seismic rates is not yet sufficiently accurate for our purposes, giving $m_{\max}$ in the range of 8.5 to 9.7, comparing these estimates to the number of largest earthquakes in the subduction zones during the last 110 years definitely argues for the larger of the above values.

In conclusion, we would like to determine the upper magnitude limit for the subduction zones as well as recurrence intervals for such earthquakes. For the tapered G-R (TGR) distribution Bird and Kagan (2004, Table 5) determined that $m_{cm} = 9.58^{+\infty}_{-0.23}$, and the 95% upper limit $m_{cm} = 10.1$. For the sake of simplicity we take $m_{\max} = 10.0$. Calculations similar to Eq. 8 by Kagan and Jackson (2011b) can be made to obtain an approximate estimate of the average inter-earthquake period. The return period can be estimated from Fig. 1b by Kagan (2002a) or Eq. 3 as it differs from the regular G-R law: for the TGR distribution cumulative function at m_c is below the G-R line by a factor of e. Thus, for the TGR distribution, the recurrence time for the global occurrence of the $m \geq 10.0$ earthquake is about 475 years. Of course, the distributions in these calculations are extrapolated beyond the limit of their parameters' evaluation range, but the above recurrence periods provide a rough idea how big such earthquakes can be and how frequently they can occur worldwide.

For Flinn-Engdahl (Flinn *et al.*, 1974) #19 zone, which includes Japan, the $m \geq 10.0$ earthquake could repeat in about 9,000 years for the TGR distribution. The rupture length of the $m10.0$ event can be estimated from Fig. 9 by Kagan and Jackson (2011b): at about 2100 km it is comparable to the 3000 km length of zone #19. These long recurrence periods indicate that it would be difficult to find displacement traces for these earthquakes in paleo-seismic investigations.

6 Conclusions

• 1. The major cause for excessive fatalities and economic losses during the worst global natural disaster in the Tohoku-Oki area was a gross under-estimation of the maximum earthquake magnitude ($m_{\max}$) and its recurrence interval.

• 2. Long-term forecasts based on the optimal smoothing of seismicity in and around Japan suggest that the recurrence period for the $m9$ earthquakes is of the order of 350 years in the Tohoku area.

• 3. Short-term forecasts can provide time-dependent information for aftershocks occurrence. In some cases, if foreshocks are present, as in the Tohoku sequence, mainshock rates can be predicted. Therefore, these forecasts can be used for developing an operational earthquake forecasting strategy.

Acknowledgments

We are grateful to Peter Bird and Paul Davis for useful discussion and suggestions. The authors appreciate support from the National Science Foundation through grants EAR-0711515 and EAR-0944218, as well as from the Southern California Earthquake Center (SCEC). SCEC is funded by NSF Cooperative Agreement EAR-0106924 and USGS Cooperative Agreement 02HQAG0008. Publication 0000, SCEC.

References

Bird, P., and Y. Y. Kagan, 2004. Plate-tectonic analysis of shallow seismicity: apparent boundary width, beta, corner magnitude, coupled lithosphere thickness, and coupling in seven tectonic settings, *Bull. Seismol. Soc. Amer.*, **94**(6), 2380-2399, (plus electronic supplement), see also an update at
\protect\vrule width0pt\protect\href{http://peterbird.name/publications/2004_global_couplin

Brune, J. N., 1968. Seismic moment, seismicity, and rate of slip along major fault zones, *J. Geophys. Res.*, **73**, 777-784.

Ekström, G., 2007. Global seismicity: results from systematic waveform analyses, 1976-2005, in *Treatise on Geophysics*, **4**(4.16), ed. H. Kanamori, pp. 473-481, Elsevier, Amsterdam.

Ekström, G., A. M. Dziewonski, N. N. Maternovskaya and M. Nettles, 2005. Global seismicity of 2003: Centroid-moment-tensor solutions for 1087 earthquakes, *Phys. Earth planet. Inter.*, **148**(2-4), 327-351.

England, P., and J. Jackson, 2011. Uncharted seismic risk, *Nature Geoscience*, **4**, 348-349.

Flinn, E. A., E. R. Engdahl, and A. R. Hill, 1974. Seismic and geographical regionalization, *Bull. Seismol. Soc. Amer.*, **64**, 771-992.

Geller, R. J., 2011. Shake-up time for Japanese seismology, *Nature*, **472**(7344), 407-409, DOI: doi:10.1038/nature10105.

Gutenberg, B., and C. F. Richter, 1954. *Seismicity of the Earth and Associated Phenomena*, Princeton, Princeton Univ. Press., 310 pp.

Hanks, T.C., 1992. Small earthquakes, tectonic forces, *Science*, **256**, 1430-1432.

Hayes, G. P., Paul S. Earle, Harley M. Benz, David J. Wald, Richard W. Briggs the USGS/NEIC Earthquake Response Team, 2011. 88 Hours: The U.S. Geological Survey National Earthquake Information Center Response to the 11 March 2011 Mw 9.0

Tohoku Earthquake, *Seismol. Res. Lett.*, **82**(4), 481-493.

Jackson, D. D., and Y. Y. Kagan, 1999. Testable earthquake forecasts for 1999, *Seism. Res. Lett.*, **70**(4), 393-403.

Jackson, D. D., and Y. Y. Kagan, 2011. Characteristic earthquakes and seismic gaps, In *Encyclopedia of Solid Earth Geophysics*, Gupta, H. K. (Ed.), Springer, pp. 37-40, DOI 10.1007/978-90-481-8702-7.

Jordan, T. H., and L. M. Jones, 2010. Operational earthquake forecasting: some thoughts on why and how, *Seismol. Res. Lett.*, **81**(4), 571-574.

Jordan, T. H., Y.-T. Chen, P. Gasparini, R. Madariaga, I. Main, W. Marzocchi, G. Papadopoulos, G. Sobolev, K. Yamaoka, and J. Zschau, 2011. Operational earthquake forecasting – state of knowledge and guidelines for utilization, *Annals Geophysics*, **54**(4), 315-391, doi: 10.4401/ag-5350.

Kagan, Y. Y., 1997a. Seismic moment-frequency relation for shallow earthquakes: Regional comparison, *J. Geophys. Res.*, **102**(B2), 2835-2852.

Kagan, Y. Y., 1997b. Earthquake size distribution and earthquake insurance, *Communications in Statistics: Stochastic Models*, **13**(4), 775-797.

Kagan, Y. Y., 1999. Universality of the seismic moment-frequency relation, *Pure Appl. Geoph.*, **155**(2-4), 537-573.

Kagan, Y. Y., 2002a. Seismic moment distribution revisited: I. Statistical results, *Geophys. J. Int.*, **148**(3), 520-541.

Kagan, Y. Y., 2002b. Seismic moment distribution revisited: II. Moment conservation principle, *Geophys. J. Int.*, **149**(3), 731-754.

Kagan, Y. Y., 2011. Random stress and Omori's law, *Geophys. J. Int.*, **186**(3), 1347-1364, doi: 10.1111/j.1365-246X.2011.05114.x.

Kagan, Y. Y., P. Bird, and D. D. Jackson, 2010. Earthquake patterns in diverse tectonic zones of the globe, *Pure Appl. Geoph.* (*The Frank Evison Volume*), **167**(6/7), 721-741, doi: 10.1007/s00024-010-0075-3.

Kagan, Y. Y., and D. D. Jackson, 1994. Long-term probabilistic forecasting of earthquakes, *J. Geophys. Res.*, **99**, 13,685-13,700.

Kagan, Y. Y. and D. D. Jackson, 1999. Worldwide doublets of large shallow earthquakes, *Bull. Seismol. Soc. Amer.*, **89**(5), 1147-1155.

Kagan, Y. Y., and D. D. Jackson, 2000. Probabilistic forecasting of earthquakes, *Geophys. J. Int.*, **143**, 438-453.

Kagan, Y. Y. and Jackson, D. D., 2011a. Global earthquake forecasts, *Geophys. J. Int.*, **184**(2), 759-776, doi: 10.1111/j.1365-246X.2010.04857.x.

Kagan, Y. Y. and Jackson, D. D., 2011b. Tohoku Earthquake: a Surprise? Preprint, http://arxiv.org/abs/1112.5217.

Kagan, Y., and L. Knopoff, 1977. Earthquake risk prediction as a stochastic process, *Phys. Earth Planet. Inter.*, **14**(2), 97-108, doi: 10.1016/0031-9201(77)90147-9.

Koketsu, K., and Y. Yokota, 2011. Supercycles along the Japan Trench and Foreseeability of the 2011 Tohoku Earthquake, AGU Fall Meet. Abstract U33C-03.

Matthews, M. V., W. L. Ellsworth, and P. A. Reasenberg, 2002. A Brownian model for recurrent earthquakes, *Bull. Seismol. Soc. Amer.*, **92**, 2233-2250.

Michael, A. J., 2011. Random variability explains apparent global clustering of large earthquakes, *Geophys. Res. Lett.*, **38**, L21301, doi:10.1029/2011GL049443.

Molchan, G. M., and Y. Y. Kagan, 1992. Earthquake prediction and its optimization, *J. Geophys. Res.*, **97**(B4), 4823-4838, doi:10.1029/91JB03095.

Nettles, M., Ekström, G., and H. C. Koss, 2011. Centroid-moment-tensor analysis of the

2011 off the Pacific coast of Tohoku Earthquake and its larger foreshocks and aftershocks, *Earth Planets Space*, **63**(7), 519-523.

Simons, M., Minson, S.E., Sladen, A., Ortega, F., Jiang, J.L., Owen, S.E., Meng, L.S., Ampuero, J.P., Wei, S.J., Chu, R.S., Helmberger, D.V., Kanamori, H., Hetland, E., Moore, A.W., Webb, F.H., 2011. The 2011 magnitude 9.0 Tohoku-Oki earthquake: mosaicking the megathrust from seconds to centuries, *Science*, **332**(6036), 1421-1425 DOI: 10.1126/science.1206731.

Stein, S., and E. A. Okal, 2011. The size of the 2011 Tohoku earthquake need not have been a surprise, *Eos Trans. AGU*, **92**(27), 227-228.

Stein, S., Geller, R., and Liu, M., 2011. Bad assumptions or bad luck: why earthquake hazard maps need objective testing, *Seismol. Res. Lett.*, **82**(5), 623-626.

Uchida, N., and T. Matsuzawa, 2011. Coupling coefficient, hierarchical structure, and earthquake cycle for the source area of the 2011 off the Pacific coast of Tohoku earthquake inferred from small repeating earthquake data, *Earth Planets Space*, **63**(7), 675-679.

van Stiphout, T., S. Wiemer, and W. Marzocchi (2010). Are short-term evacuations warranted? Case of the 2009 L'Aquila earthquake, *Geophys. Res. Lett.*, **37**, L06306, doi:10.1029/2009GL042352.

Wyss, M., 1973. Towards a physical understanding of the earthquake frequency distribution, *Geophys. J. R. Astr. Soc.*, **31**, 341-359.

Table 1: Examples of long- and short-term forecast during the Tohoku earthquake sequence.

Lati-tude	Longi-tude	LONG-TERM FORECAST						SHORT-TERM	
		Probability	Focal mechanism					Probability	Probability
		$m \geq 5.8$	T-axis		P-axis		Rotation	$m \geq 5.8$	ratio
		eq/day*km^2	Pl	Az	Pl	Az	angle	eq/day*km^2	Time-
							degree	Time-	dependent/
								dependent	independent
March 8									
141.0	38.5	1.64E-08	81	307	8	107	24.31	5.603E-10	3.423E-02
141.5	38.5	2.31E-08	76	327	11	107	29.62	8.171E-10	3.535E-02
142.0	38.5	1.04E-07	76	0	5	112	31.68	4.414E-09	4.234E-02
142.5	38.5	7.60E-08	63	312	25	113	11.78	2.667E-09	3.510E-02
143.0	38.5	4.98E-08	60	303	29	113	10.25	1.215E-09	2.441E-02
143.5	38.5	3.06E-08	61	303	28	113	13.13	5.691E-10	1.861E-02
144.0	38.5	1.77E-08	61	306	28	114	15.54	1.240E-10	6.993E-03
144.5	38.5	1.21E-08	55	292	35	117	27.55	3.989E-10	3.300E-02
145.0	38.5	2.08E-08	7	275	82	62	27.84	1.238E-09	5.953E-02
March 10									
141.0	38.5	1.64E-08	81	307	8	107	24.34	5.880E-10	3.583E-02
141.5	38.5	2.32E-08	76	327	11	107	29.56	1.406E-08	0.605
142.0	38.5	1.05E-07	76	360	6	112	31.66	2.482E-06	23.7
142.5	38.5	8.14E-08	63	311	26	113	11.82	7.895E-06	97.0
143.0	38.5	5.87E-08	60	301	30	113	9.76	5.298E-06	90.2
143.5	38.5	3.67E-08	61	303	28	113	11.19	1.868E-06	50.9
144.0	38.5	1.78E-08	61	305	28	114	15.47	2.314E-07	13.0
144.5	38.5	1.21E-08	55	292	35	117	27.45	3.644E-09	0.301
145.0	38.5	2.08E-08	7	275	82	63	27.91	1.241E-09	5.963E-02
March 11									
141.0	38.5	1.64E-08	81	307	8	107	24.35	4.960E-06	303
141.5	38.5	2.33E-08	76	326	11	107	29.51	9.397E-06	404
142.0	38.5	1.05E-07	75	359	6	112	31.64	4.938E-05	471
142.5	38.5	8.32E-08	63	310	26	113	11.80	4.271E-05	514
143.0	38.5	6.32E-08	59	301	30	113	9.47	3.109E-05	492
143.5	38.5	4.10E-08	61	302	29	113	10.75	1.978E-05	482
144.0	38.5	2.03E-08	60	304	29	117	14.44	9.430E-06	466
144.5	38.5	1.33E-08	55	293	35	117	25.04	5.504E-06	413
145.0	38.5	2.14E-08	9	275	81	74	29.44	6.765E-06	316

Table 2: Pairs of shallow earthquakes $m \geq 7.5$

	First Event				Second Event				Difference			
No	Date	Coord.		m	Date	Coord.		m	R	Φ	Δt	η
		Lat.	Long.			Lat.	Long.		km	°	day	
1	1977/06/22	-22.9	-174.9	8.1	2009/03/19	-23.1	-174.2	7.7	75	55	11593.26	1.4
2	1978/03/23	44.1	149.3	7.6	1978/03/24	44.2	149.0	7.6	25	7	1.69	2.3
3	1978/06/12	38.0	142.1	7.7	2011/03/11	37.5	143.1	9.2	104	12	11959.90	4.4
4	1980/07/08	-12.9	166.2	7.5	1980/07/17	-12.4	165.9	7.8	62	18	8.85	1.1
5	1980/07/08	-12.9	166.2	7.5	1997/04/21	-13.2	166.2	7.8	33	42	6130.53	2.0
6	1980/07/08	-12.9	166.2	7.5	2009/10/07	-12.6	166.3	7.7	37	13	10682.95	1.6
7	1980/07/17	-12.4	165.9	7.8	2009/10/07	-12.6	166.3	7.7	41	14	10674.10	1.8
8	1980/07/17	-12.4	165.9	7.8	2009/10/07	-11.9	166.0	7.9	65	12	10674.11	1.3
9	1983/03/18	-4.9	153.3	7.8	2000/11/16	-4.6	152.8	8.1	83	72	6452.83	1.3
10	1983/03/18	-4.9	153.3	7.8	2000/11/16	-5.0	153.2	7.9	47	91	6452.94	1.8
11	1985/09/19	17.9	-102.0	8.0	1985/09/21	17.6	-101.4	7.6	71	14	1.51	1.3
12	1987/03/05	-24.4	-70.9	7.6	1995/07/30	-24.2	-70.7	8.1	33	7	3068.83	2.8
13	1990/04/18	1.3	123.3	7.7	1991/06/20	1.0	123.2	7.6	37	29	427.65	1.6
14	1995/08/16	-5.5	153.6	7.8	2000/11/16	-5.0	153.2	7.9	76	74	1918.89	1.1
15	1997/04/21	-13.2	166.2	7.8	2009/10/07	-12.6	166.3	7.7	70	30	4552.42	1.0
16	2000/06/04	-4.7	101.9	7.9	2007/09/12	-3.8	101.0	8.6	150	85	2655.78	1.3
17	2000/11/16	-4.6	152.8	8.1	2000/11/16	-5.0	153.2	7.9	67	89	0.12	1.7
18	2000/11/16	-4.6	152.8	8.1	2000/11/17	-5.3	152.3	7.8	93	88	1.67	1.2
19	2001/06/23	-17.3	-72.7	8.5	2001/07/07	-17.5	-72.4	7.7	34	8	13.54	4.7
20	2005/03/28	1.7	97.1	8.7	2010/04/06	2.0	96.7	7.8	58	7	1835.25	4.0
21	2006/11/15	46.7	154.3	8.4	2007/01/13	46.2	154.8	8.2	70	82	58.71	2.7
22	2007/09/12	-3.8	101.0	8.6	2007/09/12	-2.5	100.1	7.9	176	11	0.53	1.2
23	2007/09/12	-3.8	101.0	8.6	2010/10/25	-3.7	99.3	7.9	189	8	1139.15	1.1
24	2011/03/11	37.5	143.1	9.2	2011/03/11	35.9	141.4	8.0	232	7	0.020	2.1
25	2011/03/11	37.5	143.1	9.2	2011/03/11	38.3	144.6	7.7	162	62	0.027	2.9

Notes: R – centroid distance, Φ – 3-D rotation angle between focal mechanisms, Δt – time interval between events, η – degree of zone overlap, the ratio of earthquake focal zone sizes to twice their distance, see Equations (2,3) in Kagan and Jackson (1999). The total earthquake number with magnitude $m \geq 7.50$ for the period 1976/1/1–2011/09/20 is 126. The maximum epicentroid distance is 250.0018km.

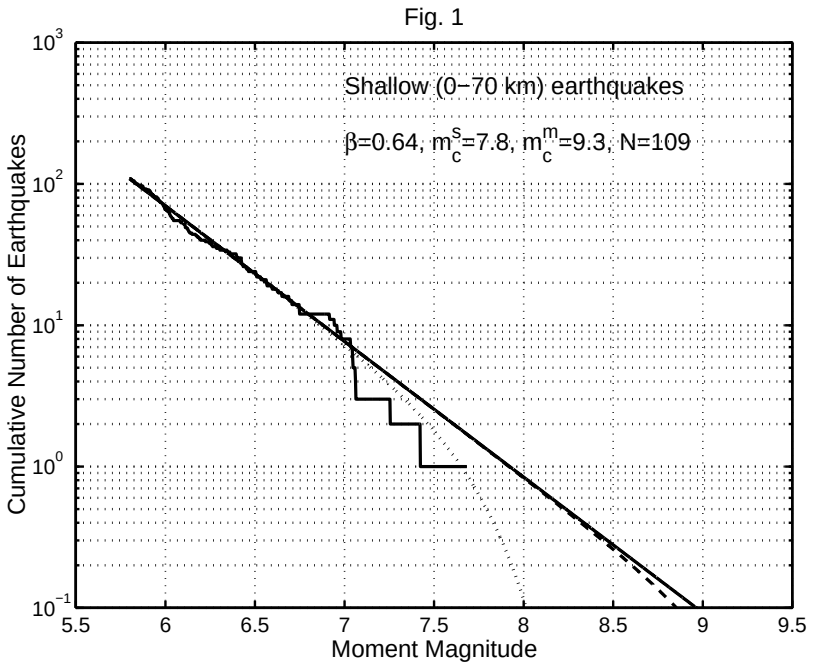

Figure 1:

The number of earthquakes in the Tohoku area (35-40° N, 140-146° E) with the moment magnitude (m) larger than or equal to m as a function of m for the shallow earthquakes in the GCMT catalog during 1977–2010. Magnitude threshold $m_t = 5.8$, the total number of events is 109. The unrestricted Gutenberg-Richter law is shown by a solid line. Dashed and dotted lines show two tapered G-R distributions: the G-R law restricted at large magnitudes by an exponential taper with a corner magnitude. One corner magnitude $m_c^s = 7.8$ is evaluated by the maximum likelihood method using the earthquake statistical record, another estimate $m_c^m = 9.3$ is based on the moment conservation. The slope of the linear part of the curve corresponds to $\beta = 0.640$.

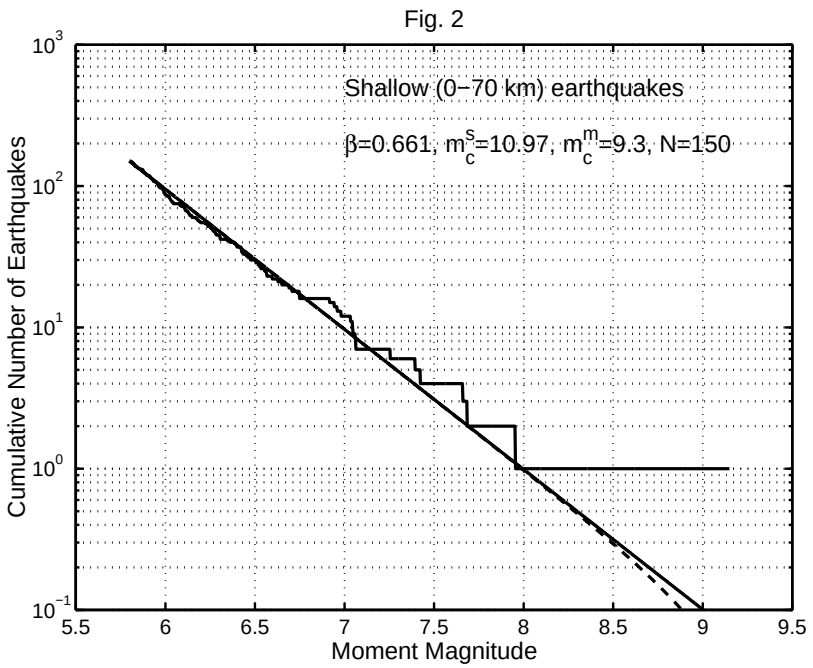

Figure 2:

Magnitude-frequency relation for the Tohoku area. The plot is similar to Fig. 1, but the time interval is 1977–2011; the total number of events is 150. One corner magnitude $m_c^s = 10.97$ is evaluated by the maximum likelihood method, another estimate $m_c^m = 9.3$ is based on the moment conservation (Kagan and Jackson, 2011b). The slope of the linear part of the curve corresponds to $\beta = 0.661$. Because of the high value of the corner magnitude ($m_c^s = 10.97$), one of the curves for the TGR distribution practically overlays the G-R straight line.

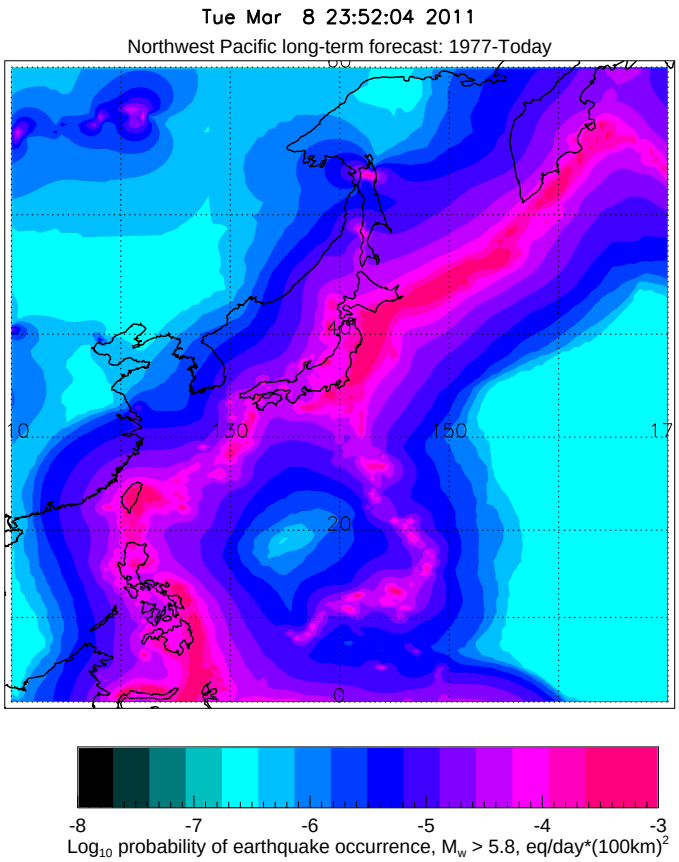

Figure 3:

The long-term forecast rate for the north-west (NW) Pacific calculated March 8, 2011, before the $m7.4$ Tohoku foreshock.

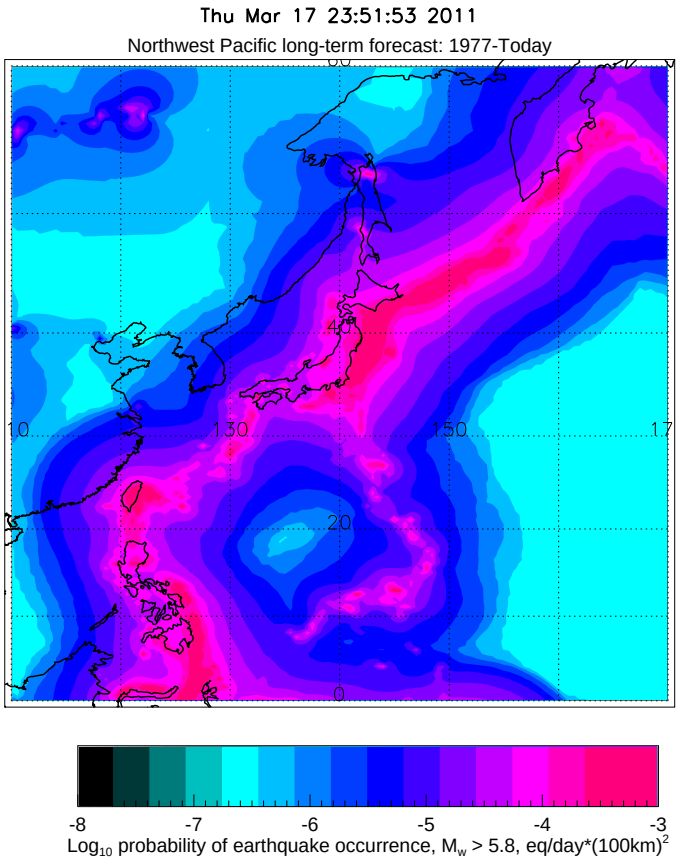

Figure 4:

The long-term forecast rate for the NW Pacific calculated March 17, 2011, after the Tohoku mainshock. There is little change compared to Fig. 3.

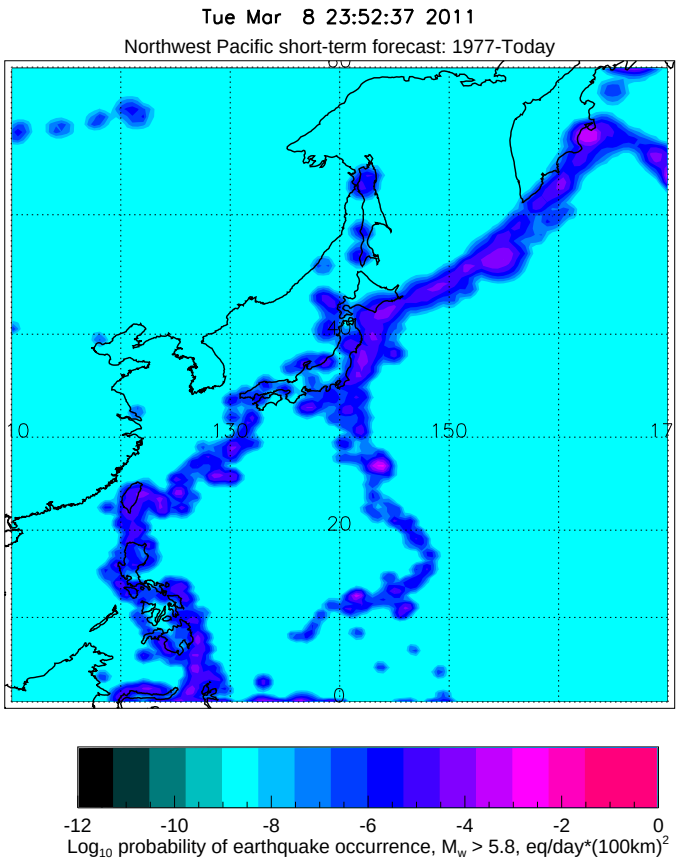

Figure 5:

The short-term forecast rate for the NW Pacific calculated March 8, 2011, before the $m7.4$ foreshock.

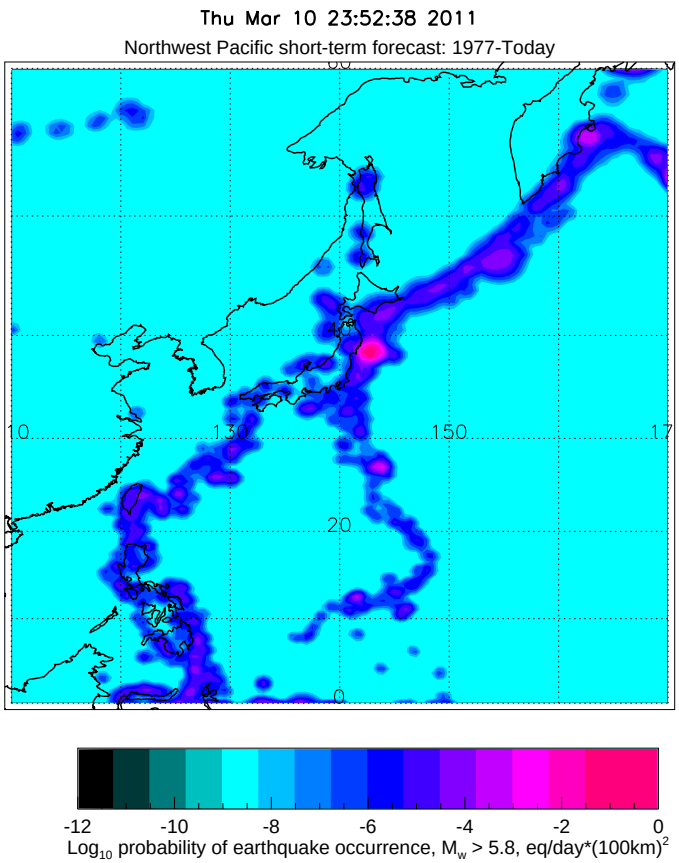

Figure 6:

The short-term forecast rate for the NW Pacific calculated March 10, 2011, after the $m7.4$ foreshock, just before the Tohoku $m9.1$ mainshock – at the foreshock epicenter the short-term rates are about 100 times higher than the long-term rates.

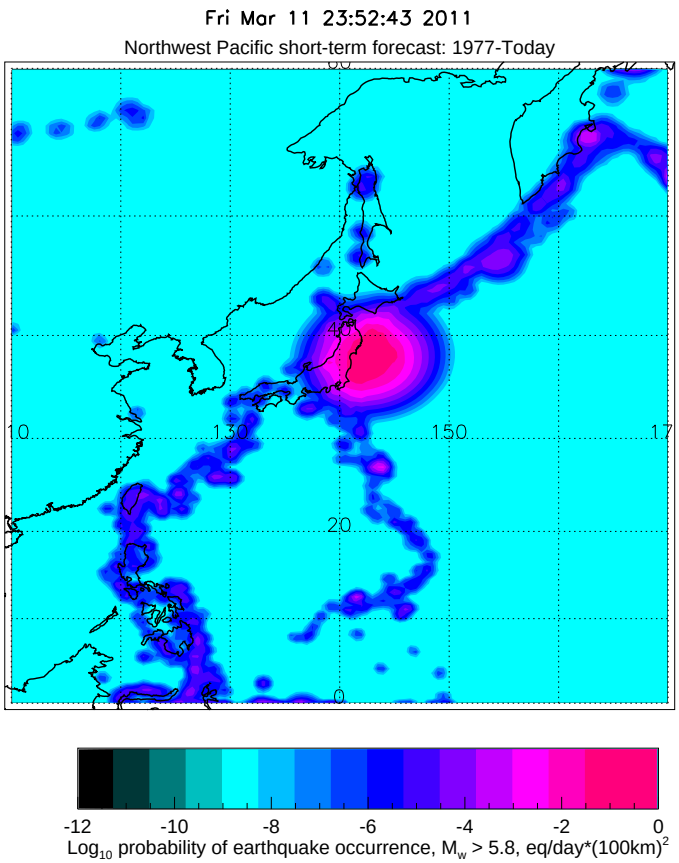

Figure 7:

The short-term forecast rate for the NW Pacific calculated March 11, 2011, immediately after the $m9.1$ mainshock, the short-term rates are about 1000 times higher than the long-term rates.

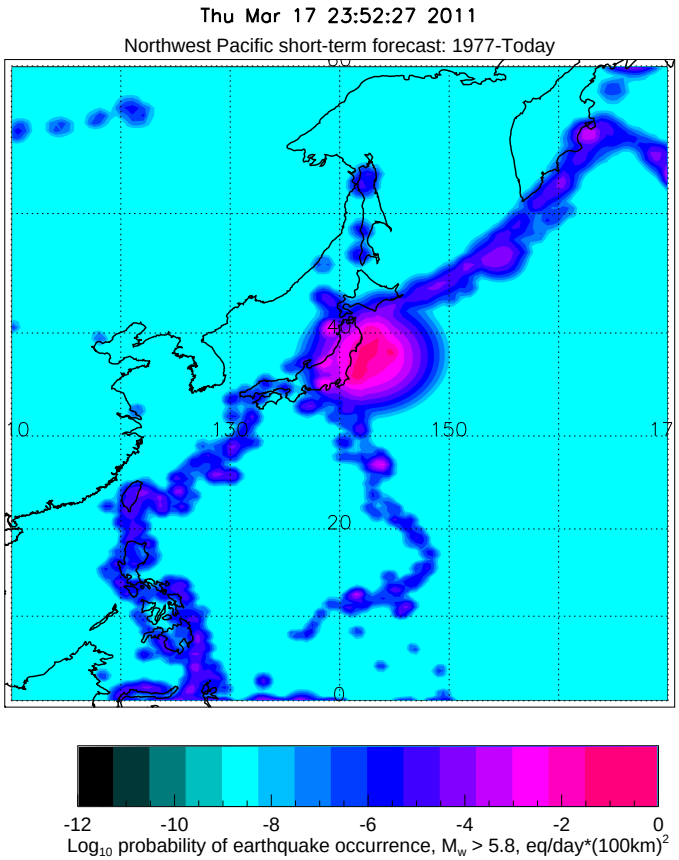

Figure 8:

The short-term forecast rate for the NW Pacific calculated March 17, 2011, a week after the $m9.1$ mainshock, the short-term rates are about 100 times higher than the long-term rates.